Inorganic Chemistry
Article

Inorg. Chem. **2010**, *49*, 1983–1994 **1983**
DOI: 10.1021/ic9024487

Efficient Syntheses of 5-X-$B_{10}H_{13}$ Halodecaboranes via the Photochemical (X = I) and/or Base-Catalyzed (X = Cl, Br, I) Isomerization Reactions of 6-X-$B_{10}H_{13}$

William C. Ewing, Patrick J. Carroll, and Larry G. Sneddon*

Department of Chemistry, University of Pennsylvania, Philadelphia, Pennsylvania 19104-6323

Received December 9, 2009

High yield syntheses of the 5-X-$B_{10}H_{13}$ (**5X**) halodecaboranes have been achieved through the photochemical (X=I) or base-catalyzed (X=Cl, Br, I) isomerization reactions of their 6-X-$B_{10}H_{13}$ (**6X**) isomers. **5I** was obtained in 80% isolated yield upon the UV photolysis of **6I**. Treatment of **6X** (X=Cl, Br, I) with catalytic amounts of triethylamine at 60 °C led to the formation of 78:22 (Cl), 82:18 (Br), and 86:14 (I) ratio **5X**/**6X** equilibrium mixtures. The **5X** isomers were then separated from these mixtures by selective crystallization (Br and I) or column chromatography (Cl), with the supernatant mixtures in each case then subjected to another round of isomerization/separation to harvest a second crop of **5X**. The combined isolated yields of pure products after two cycles were 71% 5-Cl-$B_{10}H_{13}$, 83% 5-Br-$B_{10}H_{13}$, and 68% 5-I-$B_{10}H_{13}$. The previously proposed structures of 5-Br-$B_{10}H_{13}$ and 5-I-$B_{10}H_{13}$ were crystallographically confirmed. Deprotonation of **6X** and **5X** with 1,8-bis(dimethylamino)naphthalene (PS) resulted in the formation of [PSH^+][**6X**$^-$] and [PSH^+][**5X**$^-$]. Density functional theory-gauge-independent atomic orbital (DFT/GIAO) calculations and crystallographic determinations of [PSH^+][**6Cl**$^-$] and [PSH^+][**6Cl**$^-$] confirmed bridge-deprotonation at a site adjacent to the halogen-substituted borons. NMR studies of the 6-Br-$B_{10}H_{13}$ isomerization induced by stoichiometric amounts of PS showed that following initial deprotonation to form 6-Br-$B_{10}H_{12}^-$, isomerization occurred at 60 °C to form an equilibrium mixture of 6-Br-$B_{10}H_{12}^-$ and 5-Br-$B_{10}H_{12}^-$. DFT calculations also showed that the observed 5-X-$B_{10}H_{13}$/6-X-$B_{10}H_{13}$ equilibrium ratios in the triethylamine-catalyzed reactions were consistent with the energetic differences of the 5-X-$B_{10}H_{12}^-$ and 6-X-$B_{10}H_{12}^-$ anions. These results strongly support a mechanistic pathway for the base-catalyzed **6X** to **5X** conversions involving the formation and subsequent isomerizations of the **6X**$^-$ anions. While triethylamine did not catalyze the isomerization reactions of either 6-(C_6H_{13})-$B_{10}H_{13}$ or 6,9-(C_6H_{13})$_2$-$B_{10}H_{12}$, it catalyzed the isomerization of 6-X-9-(C_6H_{13})-$B_{10}H_{12}$ to 5-X-9-(C_6H_{13})-$B_{10}H_{12}$ resulting from halo, but not alkyl rearrangement. Comparisons of the chemical shift values found in the temperature-dependent ^{11}B NMR spectra of **6Cl**$^-$ and **6F**$^-$ with DFT/GIAO chemical shift calculations indicate the fluxional behavior observed for these anions results from a process involving hydrogen migration around the open face that leads to the averaging of some boron resonances at higher temperatures.

Introduction

Decaborane ($B_{10}H_{14}$) is the most widely available neutral polyborane and is a key starting material for the production of numerous polyborane compounds having applications in fields ranging from materials to medicine.[1,2] The incorporation of decaborane into a wider range of more complex molecules with tuned properties will depend upon the development of new efficient methods for its selective functionalization. Recently, we reported simple, high yield syntheses of the 6-X-$B_{10}H_{13}$ (**6X**) (X = F, Cl, Br, I)[3] halodecaboranes by the cage-opening reactions of *closo*-$B_{10}H_{10}^{2-}$ salts. Since *closo*-$B_{10}H_{10}^{2-}$ can be prepared through the pyrolysis of borohydrides,[4] rather than from the hazardous diborane pyrolysis generally employed for the synthesis of the parent decaborane, halodecaboranes prepared by this route could prove attractive alternative starting materials for decaborane-based syntheses.

The 5-X-$B_{10}H_{13}$ (**5X**) (X = Cl, Br, I) halodecaboranes have previously[5,6] been produced in low yields as mixtures with

*To whom correspondence should be addressed. E-mail: lsneddon@sas.upenn.edu.

(1) (a) Plesek, J. *Chem. Rev.* **1992**, *92*, 269–278. (b) Packirisamy, S. *Prog. Polym. Sci.* **1996**, *21*, 707–773. (c) Wei, X.; Carroll, P. J.; Sneddon, L. G. *Chem. Mater.* **2006**, *18*, 1113–1123. (d) Teixidor, F.; Vinas, C.; Demonceau, A.; Nunez, R. *Pure Appl. Chem.* **2003**, *75*, 1305–1313. (e) Grimes, R. N. *J. Chem. Educ.* **2004**, *81*, 657–672.

(2) (a) Hawthorne, M. F. *Angew. Chem., Int. Ed. Engl.* **1993**, *32*, 950–984. (b) Barth, R. F.; Soloway, A. H.; Fairchild, R. G. *Sci. Am.* **1990**, 100–107. (c) Soloway, A. H.; Tjarks, W.; Barnum, B. A.; Rong, F.-G.; Barth, R. F.; Codogni, I. M.; Wilson, J. G. *Chem. Rev.* **1998**, *98*, 1515–1562.

(3) Ewing, W. C.; Carroll, P. J.; Sneddon, L. G. *Inorg. Chem.* **2008**, *47*, 8580–8582.

(4) (a) Colombier, M.; Atchekzai, J.; Mongeot, H. *Inorg. Chim. Acta* **1986**, *115*, 11–16. (b) Makhlouf, J. M.; Hough, W. V.; Hefferan, G. T. *Inorg. Chem.* **1967**, *6*, 1196–1198.

(5) (a) Plesek, J.; Stibr, B.; Hermanek, S. *Collect. Czech. Chem. Commun.* **1966**, *31*, 4744–4745. (b) Stibr, B.; Plesek, J.; Hermanek, S. *Collect. Czech. Chem. Commun.* **1969**, *34*, 194–205.

(6) Sprecher, R. F.; Aufderhiede, B. E.; Luther, G. W., III; Carter, J. C. *J. Am. Chem. Soc.* **1974**, *96*, 4404–4410.

Published on Web 01/21/2010

their 6-X-$B_{10}H_{13}$ isomers. For example, the reactions of 6,9-$(Me_2S)_2$-$B_{10}H_{12}$ with anhydrous HCl and HBr yielded 5:95 **5Cl**/**6Cl** and 20:80 **5Br**/**6Br** mixtures in 60% and 96% yields, respectively. Separation of the minor 5-X-$B_{10}H_{13}$ products in these mixtures was then achieved by preparative thin layer chromatography, but isolated yields of the pure products were not reported.[6] An earlier paper reported **5Br** yields of ~30% following column chromatographic separation of a 43:57 ratio **5Br**/**6Br** mixture generated using the same HBr reaction.[7] The reaction of 6,9-$(Me_2S)_2$-$B_{10}H_{12}$ with HI gave a much more favorable, 63:37, **5I**/**6I** ratio, but with only a low 16% total yield of the monoiododecaborane mixture.[6] Herein we now report simple photochemical and/or base-catalyzed isomerization reactions of 6-X-$B_{10}H_{13}$ that provide the first efficient synthetic routes to the 5-X-$B_{10}H_{13}$ (X = Cl, Br, I) halodecaboranes, making these chiral, functionalized boranes readily available for use in the construction of decaborane-based compounds and materials.

Experimental Section

General Synthetic Procedures and Materials. The decaborane-derivatives, 6-F-$B_{10}H_{13}$ (**6F**),[3] 6-Cl-$B_{10}H_{13}$ (**6Cl**),[3] 6-Br-$B_{10}H_{13}$ (**6Br**),[3] 6-I-$B_{10}H_{13}$ (**6I**),[3] 6-(C_6H_{13})-$B_{10}H_{13}$[8] and 6,9-$(C_6H_{13})_2$-$B_{10}H_{12}$,[9] were prepared by the literature methods. Tetrabutylammonium chloride (Fluka) was azeotropically dried with toluene and stored in an inert environment. Proton Sponge (1,8-bis(dimethylamino)naphthalene, Aldrich) was sublimed prior to use and stored away from light. Triethylamine and pentane (Fisher) were dried over CaH_2 and distilled prior to use. Dichlorobenzene and chlorobenzene (Fisher) were dried over CaH_2, filtered, and stored in a N_2 filled drybox. Toluene was dried by passing through an activated alumina column prior to use. Propylamine, diisopropylethylamine, dibutylsulfide (Aldrich), triphenylphosphine, $PtBr_2$ (Strem), and 1-hexene (Acros) were used as received. All other solvents were used as received unless noted otherwise. Silica gel (Fisher) was pretreated with acetic acid vapors and dried in vacuo as described elsewhere.[7]

Physical Methods. ^{11}B NMR at 128.3 MHz and ^{1}H NMR at 400.1 MHz spectra were obtained on a Bruker DMX-400 spectrometer equipped with appropriate decoupling accessories. All ^{11}B chemical shifts are referenced to $BF_3 \cdot OEt_2$ (0.0 ppm), with a negative sign indicating an upfield shift. All proton chemical shifts were measured relative to internal residual protons from the lock solvents (99.9% $CDCl_3$) and then referenced to $(CH_3)_4Si$ (0.0 ppm). High- and low-resolution mass spectra employing chemical ionization with negative ion detection were obtained on a Micromass AutoSpec high-resolution mass spectrometer. IR spectra were obtained on a Perkin-Elmer Spectrum 100 FT-IR spectrometer. Melting points were determined using a standard melting point apparatus and are uncorrected. Ultraviolet irradiation was performed with a water-cooled 450 W medium-pressure Hanovia lamp.

Photolytic Reactions. 5-I-$B_{10}H_{13}$. In a N_2 filled drybox, **6I** (30.0 mg, 0.12 mmol) was dissolved in dry, degassed pentane (3 mL) in a 10 mL quartz tube equipped with a stirbar and Schlenk adapter. The stirred, room temperature solution was then subjected to UV-irradiation for 12 h. The solution turned slightly pink, and a small amount of white precipitate appeared. Analysis by ^{11}B NMR showed quantitative conversion to **5I**. The solution was filtered, concentrated, and the product recrystallized from pentane (2 mL) at −78 °C to give 24 mg (0.10 mmol, 80%) of pure **5I**. For **5I**: mp 56−58 °C (lit. 56.5−57.5 °C).[6] The ^{11}B NMR[6] and IR[10] spectra of **5I** were consistent with those previously reported. ^{1}H{^{11}B} NMR (400.1 MHz, $CDCl_3$): δ 4.18 (s, 1H), 4.08 (s, 1H), 4.01 (s, 1H), 3.51 (s, 2H), 3.37 (s, 1H), 3.17 (s, 1H), 1.25 (s, 1H), 0.83 (s, 1H), −0.39 (s, 1H), −1.50 (s, 2H), −1.92 (s, 1H).

Photolysis of 6Br and 6Cl. No isomerization was observed by ^{11}B NMR when separate solutions of **6Br** (30 mg, 0.15 mmol) and **6Cl** (30 mg, 0.19 mmol) in dry, degassed pentane (3 mL) were UV-irradiated for 24 h.

Base-Catalyzed Reactions. 5-I-$B_{10}H_{13}$ (5I). A 100 mL round-bottom flask equipped with a side arm and stirbar was charged with **6I** (785 mg, 3.16 mmol) and dry toluene (20 mL) under dry N_2 on a Schlenk line. The solution was rapidly stirred while triethylamine (8 μL, 0.06 mmol, 3 mol %) was added. The flask was sealed, and the solution stirred at 60 °C for 4 h at which point ^{11}B NMR analysis showed 86% conversion to **5I**. The solution was cooled at 0 °C while the toluene was removed in vacuo. The addition of hexanes (20 mL) to the remaining material caused the separation of a yellow oil from the hexanes layer. The yellow oil was washed 2 times with hexanes (10 mL). The hexanes layers were collected, filtered, and concentrated to give a yellowish solid (704 mg). This solid was recrystallized twice from hexanes (5 mL) at −40 °C to give pure **5I** (468 mg, 1.89 mmol) as a pale yellow solid. The supernatant solution from the crystallization, which was shown by ^{11}B NMR analysis to contain a mixture of **5I** and **6I**, was held at 0 °C and concentrated in vacuo. The resulting yellow solid was dissolved in dry toluene (10 mL) and subjected to a second isomerization by reaction with triethylamine (3−4 μL, 0.02 mmol) at 60 °C for 12 h. Workup as described above yielded a second crop of **5I** (70 mg, 0.28 mmol). The total yield of the pure pale yellow solid **5I**, isolated after 2 isomerizations was 538 mg (2.33 mmol, 68%).

An alternative synthesis of **5I** employed a combined triethylamine (TEA)-catalyzed/photolytic method. A solution of **6I** (500 mg, 2.02 mmol) in dry toluene (20 mL) was reacted with triethylamine (8 μL, 0.06 mmol, 3%) at 60 °C for 4 h, and worked up as in the first step of the TEA catalyzed synthesis of **5I** described above to give an initial yield of 309 mg (1.25 mmol) of pure **5I**. The supernatant solution from the recrystallization, which was shown by ^{11}B NMR to be a mixture of **6I** and **5I**, was then transferred to a 50 mL quartz tube and photolyzed for 24 h. An additional crop of **5I** (101 mg, 0.40 mmol) was then collected. The combined yield from the two-step TEA/photolytic reaction was 410 mg (1.65 mmol, 82%) of pure **5I**.

5-Br-$B_{10}H_{13}$ (5Br). Analysis by ^{11}B NMR showed 82% conversion to **5Br** after a solution of **6Br** (400 mg, 2.00 mmol) in dry toluene (20 mL) was reacted with triethylamine (8 μL, 0.06 mmol, 3 mol %) for 6 h at 60 °C. The mixture was cooled at 0 °C while the toluene was removed in vacuo. The addition of pentane (20 mL) caused the formation of a small amount of white precipitate. The pentane solution was filtered and concentrated at −20 °C yielding a clear oil. The oil was recrystallized twice from pentane (5.0 mL) at −78 °C yielding **5Br** (232 mg, 1.15 mmol) as a white solid. The supernatant solution from the recrystallization was concentrated at −20 °C. The resulting solid was dissolved in dry toluene (10 mL) and subjected to a second isomerization reaction with triethylamine (~2−3 μL, 0.02 mmol) for 6 h at 60 °C. Workup and recrystallization as described above yielded a second crop of **5Br** (100 mg, 0.5 mmol). The combined yield of pure **5Br**, mp 46−47 °C (lit. 46−48 °C),[6] from the two isomerization reactions was 332 mg (1.65 mmol, 83%). The ^{11}B NMR[6] and IR[10] spectra of **5Br** were consistent with those previously reported. ^{1}H{^{11}B} NMR

(7) Stuchlik, J.; Hermanek, S.; Plesek, J.; Stibr, B. *Collect. Czech. Chem. Commun.* **1970**, *35*, 339–343.
(8) Kusari, U.; Carroll, P. J.; Sneddon, L. G. *Inorg. Chem.* **2008**, *47*, 9203–9215.
(9) Mazighi, K.; Carroll, P. J.; Sneddon, L. G. *Inorg. Chem.* **1993**, *32*, 1963–1969.
(10) Sedmera, S.; Hanousek, F.; Samek, Z. *Collect. Czech. Chem. Commun.* **1968**, *33*, 2169–2176.

(400.1 MHz, $CDCl_3$): δ 4.03 (s, 2H), 3.96 (s, 1H), 3.64 (s, 1H), 3.37 (s, 1H), 3.17 (s, 2H), 1.18 (s, 1H), 0.77 (s, 1H), −0.10 (s, 1H), −1.44 (s, 1H), −1.65 (s, 1H), −1.99 (s, 1H).

5-Cl-$B_{10}H_{13}$ (5Cl). Analysis by ^{11}B NMR showed 78% conversion to **5Cl** after a solution of **6Cl** (242 mg, 1.57 mmol) in dry toluene (10 mL) was reacted with triethylamine (7 μL, 0.05 mmol, 3%) for 12 h at 60 °C. The solution was cooled at 0 °C while the toluene was removed in vacuo. After the remaining yellow oil was dissolved in a minimal amount of a 2%-CH_2Cl_2 in hexanes solution, it was chromatographed on a column containing acetic-acid treated silica gel with a 2%-CH_2Cl_2/hexanes eluent. Fractions containing only **5Cl**, as determined by ^{11}B NMR, were collected and concentrated in vacuo at −20 °C, yielding white solid **5Cl** (109 mg, 0.71 mmol, 45%), which then melted into a clear oil above 0 °C. Other fractions which contained **6Cl** and/or **5Cl/6Cl** were combined and concentrated in vacuo at −20 °C to give 100 mg (0.65 mmol) of a **5Cl/6Cl** mixture. This material was subjected to a second isomerization with triethylamine (∼2−3 μL, 0.02 mmol) for 12 h at 60 °C. Workup and chromatographic separation yielded a second crop of **5Cl** (62 mg, 0.40 mmol). The total combined yield of **5Cl** from both isomerizations was 171 mg (1.11 mmol, 71%). The ^{11}B NMR[6] spectrum of **5Cl** was consistent with that previously reported. ^{1}H{^{11}B} NMR (400.1 MHz, $CDCl_3$): δ 4.03 (s, 1H), 3.92 (s, 2H), 3.71 (s, 1H), 3.30 (s, 1H), 3.09 (s, 2H), 1.14 (s, 1H), 0.72 (s, 1H), 0.03 (s, 1H), −1.45 (s, 1H), −1.78 (s, 1H), −2.05 (s, 1H). IR (KBr, cm^{-1}) 2581 (s), 1890 (w), 1558 (w), 1497 (m), 1438 (w), 1098 (w), 1043 (w), 1012 (w), 992 (w), 960 (m), 923 (s), 880 (m), 851 (m), 808 (m), 777 (m), 740 (w), 710 (m), 654 (w), 623 (w), 599 (w), 573 (w).

Attempted Base-Promoted Isomerization of 6-F-$B_{10}H_{13}$. Analysis by ^{11}B NMR showed no evidence of isomerization after a solution of 6-F-$B_{10}H_{13}$ (150 mg, 1.07 mmol) in dry toluene (10 mL) was reacted with triethylamine (5 μL, 0.03 mmol, 3%) at 60 °C for 4 h. Even after the solution was then stirred for 15 h at 80 °C, only trace (< 2%) isomerization to 5-F-$B_{10}H_{13}$ was observed.

Isomerization of 6I with other Bases. Analysis by ^{11}B NMR of separate reactions of **6I** (200 mg, 0.80 mmol) in dry toluene (10 mL) at 60 °C under N_2 showed: (a) only trace isomerization to **5I** (< 3%) after reaction with dibutylsulfide (7 μL, 0.04 mmol, 5%) for 3 days, (b) conversion to a 60:40 **5I**/**6I** mixture after 12 h and a 85:15 **5I**/**6I** mixture after 20 h of reaction with triphenylphosphine (11 mg, 0.04 mmol, 5%), (c) conversion to 86:14 and 85:15 **5I**/**6I** mixtures when reacted with diisopropylethylamine (7 μL, 0.04 mmol, 5%) and propylamine (8 μL, 0.10 mmol, 5%) for 4 h, (d) conversion to a 87:13 **5I**/**6I** mixture when reacted with tetrabutylammonium chloride (42.0 mg, 0.15 mmol, 4 mol %) at 60 °C for 10 h.

TEA-Catalyzed Isomerization of 5I. Analysis by ^{11}B NMR showed the formation of an 86:14 ratio **5I**/**6I** mixture after **5I** (200 mg, 0.80 mmol) was reacted with triethylamine (5 μL, 0.03 mmol, 4%) for 12 h at 60 °C in dry toluene (15 mL).

TEA-Catalyzed Isomerization of 5Br. Analysis by ^{11}B NMR showed the formation of an 83:17 ratio **5Br**/**6Br** mixture after **5Br** (180 mg, 0.90 mmol) was reacted with triethylamine (5 μL, 0.03 mmol, 4%) for 12 h at 60 °C in dry toluene (15 mL).

TEA-Catalyzed Isomerization of 5Cl. Analysis by ^{11}B NMR showed the formation of a 78:22 ratio **5Cl**/**6Cl** mixture after **5Cl** (130 mg, 0.80 mmol) was reacted with triethylamine (5 μL, 0.03 mmol, 4%) for 12 h at 60 °C in dry toluene (10 mL).

Isomerization of 6-Br-$B_{10}H_{12}^-$ ($\mathbf{6Br^-}$) to 5-Br-$B_{10}H_{12}^-$ ($\mathbf{5Br^-}$). In an N_2 filled drybox, **6Br** (100 mg, 0.49 mmol) was reacted with PS (105 mg, 0.49 mmol) in 4 mL of dry dichlorobenzene to form the soluble [PSH^+][$\mathbf{6Br^-}$] salt. An aliquot of this solution was transferred to a resealable thick-walled, high-pressure NMR tube, with the isomerization of $\mathbf{6Br^-}$ to $\mathbf{5Br^-}$ then followed by ^{11}B NMR with the NMR probe heated at 60 °C. After 130 min, no further changes in the relative concentrations of the two anions were observed. The tube was opened, cooled at 0 °C, and acidified with conc. H_2SO_4 (1 drop). The ^{11}B NMR spectrum of the acidified mixture showed an 81:19 **5Br**/**6Br** ratio.

Attempted Base Isomerizations of 6-(C_6H_{13})-$B_{10}H_{13}$ and 6,9-(C_6H_{13})$_2$-$B_{10}H_{12}$. Analysis by ^{11}B NMR showed that no isomerization had occurred when separate samples of 6-(C_6H_{13})-$B_{10}H_{13}$ (200 mg, 0.97 mmol) and 6,9-(C_6H_{13})$_2$-$B_{10}H_{12}$ (200 mg, 0.69 mmol) were reacted in dry toluene (10 mL) at 60 °C for 12 h with (7 μL, 0.05 mmol, 5%) and (5 μL, 0.03 mmol, 5%) of triethylamine, respectively.

6-X-9-(C_6H_{13})-$B_{10}H_{12}$ (X = Cl, I) Syntheses. A stirred mixture of **6Cl** (115 mg, 0.74), 1-hexene (15 mL), and $PtBr_2$ (13.0 mg, 0.04 mmol) was reacted for 4 days at room temperature under N_2. The 1-hexene was removed in vacuo, and the resulting oil was dissolved in a minimal amount of hexanes. After purification by column chromatography on acetic acid treated silica gel using a 5%-CH_2Cl_2 in hexanes eluent, the eluent was removed in vacuo to give 6-Cl-9-(C_6H_{13})-$B_{10}H_{12}$ as a light-brown oil (97 mg, 0.40 mmol, 53%). For 6-Cl-9-(C_6H_{13})-$B_{10}H_{12}$: HRMS: m/z calcd for $^{12}C_6{}^1H_{25}{}^{11}B_{10}{}^{37}Cl$ 244.2545, found 244.2563. ^{11}B NMR (128.3 MHz, $CDCl_3$): δ 25.3 (s, 1B), 16.4 (s, 1B), 6.8 (d, 152, 2B), −1.9 (d, J = ∼100, 4B), −35.9 (d, J = 164, 1B), −37.9 (d, J = 148, 1B). ^{1}H{^{11}B} NMR (400.1 MHz, $CDCl_3$): δ 3.45 (s, 2H), 2.98 (s, 4H), 1.59 (m, 2H), 1.44 (m, 4H), 1.35 (m, 4H), 1.13 (s, 1H), 0.93 (t, J = 6.4, 3H), 0.70 (s, 1H), −0.61 (s, 2H), −1.34 (s, 2H). See Supporting Information, Table S43 for IR data.

An analogous reaction of **6I** (300 mg, 1.21 mmol), 1-hexene (15 mL), and $PtBr_2$ (24.0 mg, 0.06 mmol) gave 6-I-9-(C_6H_{13})-$B_{10}H_{12}$ as a light-brown oil (112 mg, 0.34 mmol, 28%). For 6-I-9-(C_6H_{13})-$B_{10}H_{12}$ HRMS: m/z calcd for $^{12}C_6{}^1H_{25}{}^{11}B_{10}{}^{127}I$ 334.1931, found 334.1948. ^{11}B NMR (128.3 MHz, $CDCl_3$): δ 26.5 (s, 1B), 9.4 (d, J = 147, 2B), 2.4 (d, J = 162, 2B), −2.5 (d, J = 148, 2B), −8.0 (s, 1B), −35.0 (d, J = 150, 1B), −36.2 (d, J = 154, 1B). ^{1}H{^{11}B} NMR (400.1 MHz, $CDCl_3$): δ 3.60 (s, 2H), 3.26 (s, 2H), 2.96 (s, 2H), 1.59 (m, 2H), 1.40 (m, 4H), 1.34 (m, 4H), 1.14 (s, 2H), 0.93 (t, J = 6.6, 3H), −0.76 (s, 2H), −1.54 (s, 2H). See Supporting Information, Table S43 for IR data.

TEA-Catalyzed Isomerizations of 6-X-9-(C_6H_{13})-$B_{10}H_{12}$ (X = Cl, I). Analysis by ^{11}B NMR showed ∼70% conversion to 5-Cl-9-(C_6H_{13})-$B_{10}H_{12}$ after reaction of 6-Cl-9-(C_6H_{13})-$B_{10}H_{12}$ (92 mg, 0.38 mmol) with triethylamine (3 μL, 0.02 mmol, 5%) in dry toluene (8 mL) under N_2 for 18 h at 60 °C and ∼93% conversion to 5-I-9-(C_6H_{13})-$B_{10}H_{12}$ after reaction of 6-I-9-(C_6H_{13})-$B_{10}H_{12}$ (84 mg, 0.25 mmol) with triethylamine (∼2 μL, 0.01 mmol, 5%) in dry toluene (6 mL) under N_2 for 4 h at 60 °C. In both cases, the toluene was removed in vacuo, and the remaining light-brown oil was dissolved in a minimal amount of 2%-CH_2Cl_2 in hexanes. Chromatographic separations on acetic acid treated silica gel with 2%-CH_2Cl_2 in hexanes elution gave 5-Cl-9-(C_6H_{13})-$B_{10}H_{12}$ (40 mg, 0.17 mmol, 43%) and 5-I-9-(C_6H_{13})-$B_{10}H_{12}$ (43 mg, 0.13 mmol, 51%) as a light-brown oils. For 5-Cl-6-(C_6H_{13})-$B_{10}H_{12}$: HRMS m/z calcd for $^{12}C_6{}^1H_{25}{}^{11}B_{10}{}^{37}Cl$ 244.2545, found 244.2655. ^{11}B NMR (128.3 MHz, $CDCl_3$): δ 27.1 (s, 1B), 11.5 (s, 1B), 11.5 (d, J = ∼110, B), 10.2 (d, J = 154, 1B), 6.2 (d, J = 158, 1B), 0.8 (d, J = 145, 1B), −3.7 (d, J = ∼115, 1B), −4.3 (d, J = ∼125, 1B), −34.6 (d, J = 155, 1B), −37.4 (d, J = 159, 1B). ^{1}H{^{11}B} NMR (400.1 MHz, $CDCl_3$): δ 3.80 (s, 2H), 3.58 (s, 2H), 3.01 (s, 2H), 2.83 (s, 1H), 1.59 (m, 2H), 1.43 (m, 4H), 1.34 (bm, 4H), 0.92 (t, J = 6.1, 3H), 0.86 (s, 1H), 0.12 (s, 1H), −1.00 (s, 1H), −1.59 (s, 1H), −1.68 (s, 1H). See Supporting Information, Table S43 for IR data. For 5-I-6-(C_6H_{13})-$B_{10}H_{12}$: HRMS m/z calcd for $^{12}C_6{}^1H_{25}{}^{11}B_{10}{}^{127}I$ 334.1931, found 334.1924. ^{11}B NMR (128.3 MHz, $CDCl_3$): δ 25.9 (s, 1B), 12.3 (d, J = 160, 1B), 10.9 (d, J = ∼165, 1B), 9.0 (d, J = 153, 1B), 0.4 (d, J = 151, 1B), −0.7 (d, J = 144, 1B), −3.7 (d, J = 139, 1B), −14.0 (s, 1B), −33.8 (d, J = 156, 1B), −37.0 (d, J = 159, 1B). ^{1}H{^{11}B} NMR (400.1 MHz, $CDCl_3$): δ 4.07 (s, 2H), 3.38 (s, 2H), 3.28 (s, 1H), 2.92 (s, 1H), 1.58 (m, 2H), 1.41 (m, 4H), 1.33 (bm, 4H), 1.28 (s, 1H), 1.08 (s, 1H), 0.92

Table 1. Crystallographic Data for **5I**, **5Br**, **6Cl**$^-$, and **5Cl**$^-$

	5I	**5Br**	[PSH$^+$][**6Cl**$^-$]	[PSH$^+$][**5Cl**$^-$]
empirical formula	$B_{10}H_{13}I$	$B_{10}H_{13}Br$	$C_{14}B_{10}H_{31}N_2Cl$	$C_{14}B_{10}H_{31}N_2Cl$
formula weight	248.10	201.11	370.96	370.96
crystal class	monoclinic	orthorhombic	monoclinic	monoclinic
space group	$P2_1/c$	$Pca2_1$	$P2_1/c$	$P2_1/n$
Z	4	8	4	4
a, Å	12.803(3)	11.214(7)	9.1706(15)	9.4491(11)
b, Å	7.2932(15)	12.815(14)	23.403(4)	9.9107(9)
c, Å	10.874(2)	13.507(7)	10.1822(17)	23.784(3)
β, deg	92.308(5)		98.755(5)	97.446(3)
V, Å^3	1014.5(4)	1941(3)	2159.8(6)	2208.5(4)
D_{calc}, g/cm^3	1.624	1.376	1.141	1.116
μ, cm^{-1}	30.77	40.15	1.78	1.75
λ, Å (Mo−K$_\alpha$)	0.71073	0.71073	0.71073	0.71073
crystal size, mm	0.40 × 0.18 × 0.06	0.38 × 0.26 × 0.12	0.35 × 0.30 × 0.06	0.22 × 0.22 × 0.12
F(000)	464	784	784	784
2θ angle, deg	3.18−27.49	2.85−27.48	2.67−25.04	2.68−25.04
temperature, K	160(1)	143(1)	143(1)	143(1)
hkl collected	$-16 \le h \le 14$; $-9 \le k \le 7$; $-14 \le l \le 14$	$-12 \le h \le 14$; $-13 \le k \le 16$; $-17 \le l \le 17$	$-10 \le h \le 10$; $-27 \le k \le 25$; $-12 \le l \le 12$	$-11 \le h \le 11$; $-11 \le k \le 11$; $-28 \le l \le 28$
no. meas reflns	9143	13039	21783	31640
no. of unique reflns	2314 (R_{int} = 0.0272)	4389 (R_{int} = 0.0224)	3800 (R_{int} = 0.0364)	3895 (R_{int} = 0.0329)
no. parameters	153	200	369	369
R^a indices ($F > 2\sigma$)	R_1 = 0.0354 wR_2 = 0.0945	R_1 = 0.0379 wR_2 = 0.0870	R_1 = 0.0478 wR_2 = 0.1238	R_1 = 0.0479 wR_2 = 0.1252
R^a indices (all data)	R_1 = 0.0389 wR_2 = 0.0962	R_1 = 0.0446 wR_2 = 0.0901	R_1 = 0.0569 wR_2 = 0.1320	R_1 = 0.0550 wR_2 = 0.1320
GOF^b	1.156	1.150	1.054	1.085
final difference peaks, e/Å^3	+0.963, −1.245	+1.135, −1.381	+0.179, −0.381	+0.201, −0.289

$^a R_1 = \sum||F_o| - |F_c||/\sum|F_o|$; $wR_2 = \{\sum w(F_o^2 - F_c^2)^2/\sum w(F_o^2)^2\}^{1/2}$. ^{b} GOF = $\{\sum[w(F_o^2 - F_c^2)^2]/(n-p)\}^{1/2}$ where n = no. of reflns; p = no. of params refined.

(t, J = 6.4, 3H), −0.28 (s, 1H), −1.03 (s, 1H), −1.44 (s, 2H). See Supporting Information, Table S43 for IR data.

NMR studies of 6-X-$B_{10}H_{12}^-$ (X = Cl, F) and 5-Cl-$B_{10}H_{12}^-$ (5Cl$^-$). For lower temperature studies, **6Cl** (30 mg, 0.19 mmol), **5Cl** (30 mg, 0.19 mmol), and **6F** (25 mg, 0.18 mmol) were reacted with 1 equiv of 1,8-bis(dimethylamino)naphthalene (Proton Sponge, PS) (40 mg, 40 mg and 38 mg, respectively) in $CDCl_3$ (3 mL) to form [PSH$^+$][**6Cl**$^-$], [PSH$^+$][**5Cl**$^-$], and [PSH$^+$][**6F**$^-$], respectively, as bright yellow solutions. The NMR spectra of an aliquot of each sample were then recorded over the 32 °C to −53 °C range allowing at least 5 min for the sample to equilibrate at each new temperature. For the higher temperature studies, the same amounts of **6Cl**, **5Cl**, **6F**, and PS were reacted in chlorobenzene (3 mL), and the aliquots loaded into resealable thick-walled, high-pressure NMR tubes, with their spectra then obtained from 32 to 102 °C with the same 5 min equilibration time.

Crystallographic Data. Single crystals of **5Br** and **5I** were grown via slow solvent evaporation from heptane at −20 °C. Crystals of [PSH$^+$][**6Cl**$^-$] and [PSH$^+$][**5Cl**$^-$] grew from chlorobenzene solutions at 10 °C.

Collection and Reduction of the Data. Crystallographic data and structure refinement information are summarized in Table 1. X-ray intensity data for **5Br** (Penn3340), **5I** (Penn3334), [PSH$^+$][**6Cl**$^-$] (Penn3358), and [PSH$^+$][**5Cl**$^-$] (Penn3359) were collected on a Rigaku R-AXIS IIC area detector employing graphite-monochromated Mo−K$_\alpha$ radiation. Indexing was performed from a series of 12 0.5° rotation images with exposures of 30 s and a 36 mm crystal-to-detector distance. Oscillation images were processed using CrystalClear,[11] producing a list of unaveraged F^2 and $\sigma(F^2)$ values which were then passed to the CrystalStructure[12] program package for further processing and structure solution on a Dell Pentium III computer. The intensity data were corrected for Lorentz and polarization effects and for absorption.

Solution and Refinement of the Structures. The structures were solved by direct methods (SIR97[13]). Refinement was by full-matrix least-squares based on F^2 using SHELXL-97.[14] All reflections were used during refinement (values of F^2 that were experimentally negative were replaced with $F^2 = 0$). In the case of **5I**, [PSH$^+$][**6Cl**$^-$], and [PSH$^+$][**5Cl**$^-$] non-hydrogen atoms were refined anisotropically and hydrogen atoms were refined isotropically. In the case of **5Br**, non-hydrogen atoms were refined anisotropically, and hydrogen atoms were included as constant contributions to the structure factors and were not refined.

Computational Methods. Density Functional Theory (DFT) calculations were performed using the Gaussian 03 package.[15] All ground state, transition state, and intermediate geometries and both electronic and free energies were obtained using the

(11) *CrystalClear*; Rigaku Corporation: The Woodlands, TX, 1999.

(12) *CrystalStructure, Crystal Structure Analysis Package*; Rigaku Corp.: The Woodlands, TX , 2002.

(13) *SIR97:* Altomare, A.; Burla, M. C.; Camalli, M.; Cascarano, M.; Giacovazzo, C.; Guagliardi, A.; Moliterni, A.; Polidori, G. J.; Spagna, R. *J. Appl. Crystallogr.* **1999**, *32*, 115−119.

(14) Sheldrick, G. M. *SHELXL-97: Program for the Refinement of Crystal Structures*; University of Göttingen: Göttingen, Germany, 1997.

(15) Frisch, M. J.; Trucks, G. W.; Schlegel, H. B.; Scuseria, G. E.; Robb, M. A.; Cheeseman, J. R.; Montgomery, J. A., Jr.; Vreven, T; Kudin, K. N.; Burant, J. C.; Millam, J. M.; Iyengar, S. S.; Tomasi, J.; Barone, V.; Mennucci, B.; Cossi, M.; Scalmani, G.; Rega, N.; Petersson, G. A.; Nakatsuji, H.; Hada, M.; Ehara, M.; Toyota, K.; Fukuda, R.; Hasegawa, J.; Ishida, M.; Nakajima, T.; Honda, Y.; Kitao, O.; Nakai, H.; Klene, M.; Li, X.; Knox, J. E.; Hratchian, H. P.; Cross, J. B.; Adamo, C.; Jaramillo, J.; Gomperts, R.; Stratmann, R. E.; Yazyev, O.; Austin, A. J.; Cammi, R.; Pomelli, C.; Ochterski, J. W.; Ayala, P. Y.; Morokuma, K.; Voth, G. A.; Salvador, P.; Dannenberg, J. J.; Zakrzewski, V. G.; Dapprich, S.; Daniels, A. D.; Strain, M. C.; Farkas, O.; Malick, D. K.; Rabuck, A. D.; Raghavachari, K.; Foresman, J. B.; Ortiz, J. V.; Cui, Q.; Baboul, A. G.; Clifford, S.; Cioslowski, J.; Stefanov, B. B.; Liu, G.; Liashenko, A.; Piskorz, P.; Komaromi, I.; Martin, R. L.; Fox, D. J.; Keith, T.; Al-Laham, M. A.; Peng, C. Y.;Nanayakkara, A.; Challacombe, M.; Gill, P. M. W.; Johnson, B.; Chen, W.; Wong, M. W.; Gonzalez, C.; Pople, J. A. *Gaussian 03*, revision B.05; Gaussian, Inc.: Pittsburgh, PA, 2003.

B3LYP/6-311G(d) level without constraints for all H, C, B, and Cl atoms. Both the B3LYP/6-311G(d) level and B3LYP/SDD pseudopotential were used for Br atoms, and only the B3LYP/SDD pseudopotential was used for I atoms. The NMR chemical shifts were calculated at the B3LYP/6-311G(d) level using the gauge-independent atomic orbital (GIAO) option within Gaussian 03 and are referenced to $BF_3 \cdot O(C_2H_5)_2$ using an absolute shielding constant of 102.24 ppm. Harmonic vibrational analyses were carried out on the optimized geometries at the same level to establish the nature of stationary points. True first-order saddle points possessed only one imaginary frequency. Intrinsic reaction coordinate (IRC) calculations were carried out in both the forward and reverse directions to confirm the reaction pathways from the located transition states.

Results and Discussion

Photochemical Isomerization of 6I to 5I. UV−vis spectroscopy revealed that the **6X** and **5X** (X = Cl, Br, I) derivatives and the parent $B_{10}H_{14}$ had absorption maxima between 250 and 350 nm. However, while neither **6Br** nor **6Cl** were photochemically reactive, ^{11}B NMR analysis showed that ultraviolet irradiation of pentane solutions of ∼30−50 mg samples of **6I** for 24 h at room temperature gave quantitative conversions to **5I** (eq 1). Reaction workup with product recrystallization from cold pentane gave ∼80% isolated yields of pure **5I**.

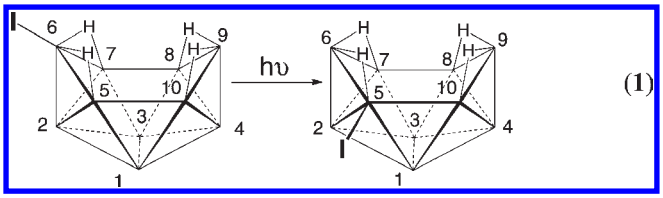

(1)

Although small scale **6I** reactions were quite suitable for **5I** syntheses, larger scale reactions proved to be less satisfactory, requiring substantially longer times and giving lower **5I** yields as a result of the formation of other unidentified side-products.

Base Catalyzed Isomerizations of 6-X-$B_{10}H_{13}$ and 5-X-$B_{10}H_{13}$. The syntheses of the 5-X-$B_{10}H_{13}$ (X = Cl, Br, I) halodecaboranes were readily achieved by treatment of their corresponding 6-X-$B_{10}H_{13}$ isomers with catalytic amounts (3%) of TEA at 60 °C (eq 2).

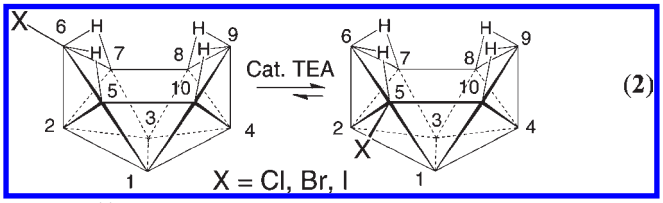

(2)

The ^{11}B NMR spectra in Figure 1 monitored the progress of the isomerization of **6I** to **5I**. Figure 1a shows the spectrum of pure **6I** immediately after the addition of TEA. The reaction can be followed by the appearance of the 5B singlet resonance of **5I** (−15.2 ppm) and the corresponding decrease of the 6B singlet resonance of **6I** (−8.2 ppm). After 20 min, (Figure 1b) the −15.2 ppm resonance was clearly evident, and after 40 min (Figure 1c) there were nearly equal amounts of **6I** and **5I**. No change in the ratio of the two isomers (∼86:14 **5I**/**6I**) was observed after 80 min (Figure 1e). Recrystallization of the mixture yielded pure **5I**, the spectrum of which is shown in Figure 1f. The supernatant solution from the recrystallization, a solution enriched in **6I**, was subjected to

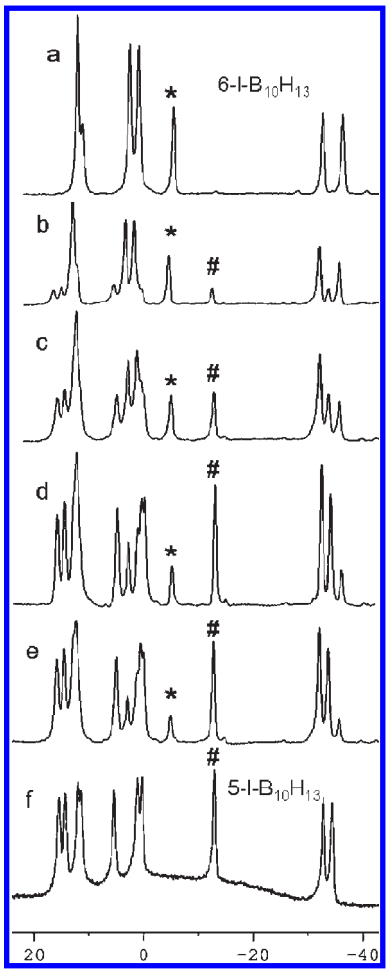

Figure 1. Isomerization of **6I** with 3 mol % TEA in toluene at 60 °C monitored by $^{11}B\{^1H\}$ NMR after: (**a**) 0 min, (**b**) 20 min, (**c**) 40 min, (**d**) 60 min, (**e**) 80 min, and (**f**) recrystallized, pure **5I**. * indicates 6-boron resonance in **6I**; # indicates 5-boron resonance in **5I**.

a second isomerization reaction with TEA and workup. The total isolated yield of **5I** after two isomerizations was 68%.

A second photolytic-step could also be used to drive the TEA-catalyzed isomerization of **6I** to completion. For example, in one experiment 500 mg of **6I** was initially isomerized with 3% TEA to yield 309 mg (62%) of recrystallized **5I**. When the supernatant material from the recrystallization, which contained a mixture of **6I** and **5I**, was then irradiated for 24 h in dry, degassed pentane, near quantitative conversion to **5I** was observed by ^{11}B NMR. Recrystallization from this solution then gave an additional 101 mg of **5I**, for a total isolated yield from the two steps of 410 mg (82%) of pure **5I**.

Both **6Br** and **6Cl** were also found to undergo TEA-catalyzed isomerizations to their **5Br** and **5Cl** isomers. After 6 h at 60 °C, ^{11}B NMR analysis of the **6Br** reaction indicated the formation of an ∼82:18 ratio **5Br**/**6Br** mixture. Separation of **5Br** by selective crystallization, followed by a second round of isomerization and crystallization of the supernatant mixture, gave a combined 83% isolated yield of **5Br**. Reaction of **6Cl** with TEA for 12 h at 60 °C produced a ∼78:22 ratio **5Cl**/**6Cl** mixture. **5Cl** was most easily separated from this mixture by column chromatography. After isolation of pure **5Cl**, fractions from the column containing **6Cl** and mixtures of **5Cl** and **6Cl** were combined and subjected to a second isomerization

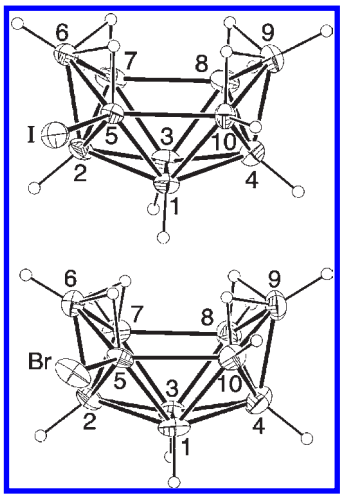

Figure 2. ORTEP drawings of the crystallographically determined structure of **5I** (top) and one of the two independent structures of **5Br** (bottom). Selected bond lengths (Å) and bond angles (deg): **5I**: B5−I, 2.166(5); B5−B6, 1.788(7); B6−B7, 1.781(9); B7−B8, 1.986(9); B8−B9, 1.784(8); B9−B10, 1.789(7); B10−B5, 1.968(7); B6−B2, 1.715(7); B9−B4, 1.729(7); I−B5−B6, 118.7(3); B2−B5−B6, 57.4(3); B4−B10−B9, 57.9(3); B5−B6−B7, 104.8(4); B8−B9−B10, 104.8(3). **5Br**: B5−Br, 1.958(4); B5−B6, 1.787(6); B6−B7, 1.766(6); B7−B8, 1.986(6); B8−B9, 1.806(7); B9−B10, 1.768(7); B10−B5, 1.978(7); B6−B2, 1.724(6); B9−B4, 1.729(7); Br−B5−B6, 120.4(3); B2−B5−B6, 57.8(2); B4−B10−B9, 58.1(3); B5−B6−B7, 104.3(3); B8−B9−B10, 105.4(3).

and chromatographic separation to ultimately give a 71% total yield of pure **5Cl**.

The melting points and ^{11}B NMR[6] and IR[10] spectra of **5I**, **5Br**, and **5Cl** match their reported values. Their ^{1}H NMR spectra are likewise consistent with the C_1 symmetry of these isomers. The **5I** and **5Br** structures were also crystallographically confirmed, as shown in the drawings in Figure 2. The halogen identity and position seem to have little effect on the bonding within a halodecaborane cage, as evidenced by the fact the corresponding cage distances and angles in **5I**, **5Br**, **6I**, and **6Br** are all quite similar. However, the B−X distances in **5Br** (1.958(4) Å and 1.945(4) Å for the two independent molecules) and **5I** (2.166(5) Å) are longer (either greater than, or just under 3σ) than those of **6Br** (1.929(4) Å) and **6I** (2.143(3) Å), respectively, suggesting less halogen π-backbonding to the cage[3] and potentially greater reactivity for **5I** and **5Br**. (See the Supporting Information, Figure S1).

When pure samples of **5Cl**, **5Br**, and **5I** were reacted for 12 h with 4 mol % of TEA in toluene at 60 °C, **5X/6X** mixtures were again produced (eq 3) with the observed isomer ratios identical to those obtained in the reactions starting with the 6-X- isomer (eq 2). This result suggests that these ratios correspond to thermodynamic equilibrium mixtures of the two isomers.

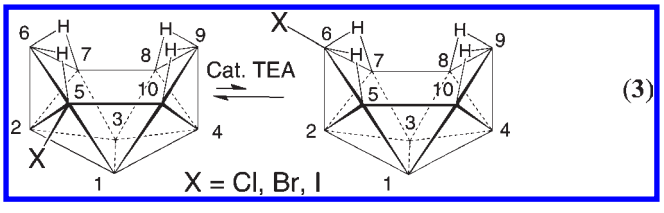

(3)

However, as can be seen in Figure 3, DFT calculations of the relative free energies of the 6-X-$B_{10}H_{13}$ and 5-X-$B_{10}H_{13}$ isomers, show that isomerization is nearly

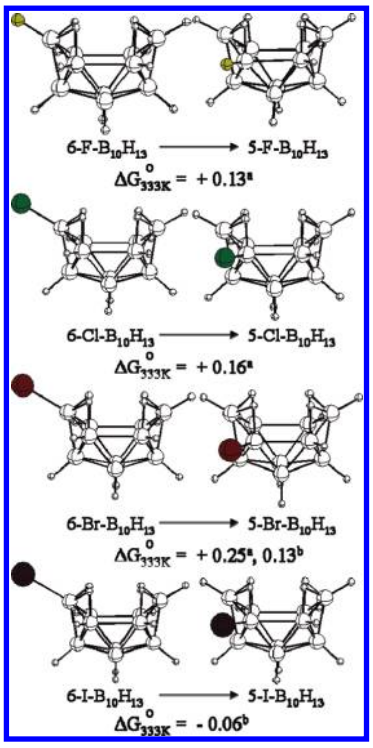

Figure 3. DFT optimized geometries of 6-X- and 5-X-$B_{10}H_{13}$ and the calculated free energy changes for the isomerization of 6-X- to 5-X-$B_{10}H_{13}$ at 60 °C. [a]Optimization and free energy calculation utilized the B3LYP/6-311G(d) basis set. [b]Optimization and free energy calculation utilized the B3LYP/6-311G(d) basis set for all H and B atoms, and the SDD pseudopotential for all halogen electrons.

energetically neutral for these compounds, with the largest energy difference of +0.25 kcal/mol for the **6Br** reaction in fact favoring the **6Br** isomer. On the basis of these calculations, an equilibrium ratio near 1:1 would have been expected rather than the observed ratios favoring the **5X** isomers.

The questions that then arise are: (1) What is the activating role of the bases in these isomerization reactions? and (2) What determines the equilibrium isomer ratio? Decaborane is known to form adducts at the B6 and B9 positions with strong Lewis bases.[16] On the other hand, strong Brønsted bases readily abstract an acidic bridging-hydrogen to produce the $B_{10}H_{13}^-$ anion.[17] A reaction of **6I** with a catalytic amount of dibutylsulfide, a strong Lewis but weak Brønsted base,[18] at 60 °C for 3 days gave only a trace of **5I**. A reaction of **6I** with triphenylphosphine, also a strong Lewis base but a somewhat better Brønsted base than dibutylsulfide,[19] reached 60% **5I** after 12 h at 60 °C and 85% **5I** after 20 h. This reaction was substantially slower than the TEA (stronger Brønsted base, pK_a = 10.68[20]) catalyzed isomerization, which was complete after only 80 min. Amines with greater (diisopropylethylamine) or lesser (propylamine) steric bulk but comparable Brønsted

(16) Hawthorne, F. M.; Pitochelli, A. R. *J. Am. Chem. Soc.* **1958**, *80*, 6685.
(17) Hawthorne, F. M.; Pitochelli, A. R.; Strahm, R. D.; Miller, J. J. *J. Am. Chem. Soc.* **1960**, *82*, 1825–1829.
(18) Bonvicini, P.; Levi, A.; Lucchini, V.; Scorrano, G. *J. Chem. Soc., Perkin Trans. 2* **1972**, 2267–2269.
(19) (a) Streuli, C. A. *Anal. Chem.* **1960**, *32*, 985–987. (b) Pestovsky, O.; Shuff, A.; Bakac, A. *Organometallics* **2006**, *25*, 2894–2898.
(20) Frenna, V.; Vivona, N.; Consiglio, G.; Spinelli, D. *J. Chem. Soc., Perkin Trans. 2* **1985**, 1865–1868.

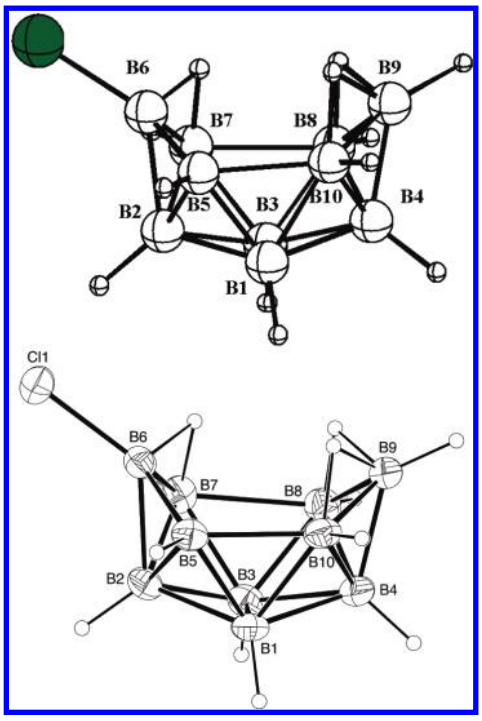

Figure 4. (top) DFT (B3LYP/6-311G(d)) optimized geometry and (bottom) crystallographically determined structure of **6Cl**$^-$. Selected bond lengths (Å) and bond angles (deg): (**top**) B6−Cl, 1.838; B5−B6, 1.645; B6−B7, 1.789; B7−B8, 2.046; B8−B9, 1.790; B9−B10, 1.800; B10−B5, 1.867; B6−B2, 1.760; B9−B4, 1.711; B2−B5, 1.820; B1−B5, 1.748; B1−B10, 1.788; B1−B4, 1.812; B3−B7, 1.771; B3−B8, 1.741; B1−B3, 1.804; Cl−B6−B2, 130.65; B7−B6−B5, 109.03; B8−B9−B10, 103.67; Cl−B6−B5, 129.41; Cl−B6−B7, 119.72; B6−B5−B10, 112.19; B6−B7−B8, 114.20; B7−B8−B9, 113.13; B5−B10−B9, 123.40. (**bottom**) B6−Cl, 1.811(2); B5−B6, 1.631(3); B6−B7, 1.781(3); B7−B8, 2.019(3); B8−B9, 1.772(4); B9−B10, 1.787(3); B10−B5, 1.862(3): B6−B2, 1.752(3); B9−B4, 1.709(3); B2−B5, 1.798(3); B1−B5, 1.738(3); B1−B10, 1.783(3); B1−B4, 1.805(3); B3−B7, 1.761(3); B3−B8, 1.742(3); B1−B3, 1.793(3); Cl−B6−B2, 129.80(14); B7−B6−B5, 108.46(16); B8−B9−B10, 103.65(15); Cl−B6−B5, 128.63(15); Cl−B6−B7, 120.70(14); B6−B5−B10, 111.47(15); B6−B7−B8, 114.84(15); B7−B8−B9, 112.95(15); B5−B10−B9, 123.83(16).

basicity[19,21] showed nearly identical rates and yields as TEA, again providing evidence that adduct formation (i.e., Lewis basicity) is not a driving force in the isomerization. Further support for this hypothesis was found by the observation that **6I** also isomerized in the presence of catalytic amounts of tetrabutylammonium chloride to form the ∼87:13 **5I**/**6I** ratio after 10 h at 60 °C. While HCl is a strong acid in water, it is only partially dissociated in many organic solvents (for example in dichloroethane: pK_a = 10.8, HCl)[22] and we have previously demonstrated that the Brønsted basicity of chloride ion is sufficient to deprotonate decaborane in organic solvents.[8] It is also significant that no halogen exchange was seen in the **6I** isomerizations with the chloride ion, providing evidence that halo dissociation/association is not a step in the halo isomerization reaction.

When the **6X** and **5X** compounds were each reacted with stoichiometric amounts of the non-nucleophilic, strong Brønsted base (pK_a ∼12) PS,[23] immediate deprotonation to form their 6-X-$B_{10}H_{12}^-$ (**6X**$^-$) and 5-X-$B_{10}H_{12}^-$ (**5X**$^-$) anions resulted. DFT calculations showed that the structures shown in Figure 4a for **6Cl**$^-$ and Figure 5a for **5Cl**$^-$, where deprotonation occurred at a site adjacent to the halogen-substituted borons, are the energetically favored isomers for these anions. As can be seen in Figures 4b and 5b, crystallographic determinations of the [PSH$^+$][**6Cl**$^-$] and [PSH$^+$][**5Cl**$^-$] salts confirmed these predictions. The intracage distances and angles in both anions are similar to those found in the crystallographic determinations of the parent [Et_3NH^+]-[$B_{10}H_{13}^-$][24] and [$PhCH_2NMe_3^+$][$B_{10}H_{13}^-$][25] salts with the unbridged B5−B6 distances (**6Cl**$^-$, 1.631(3) Å; **5Cl**$^-$, 1.644(3) Å) significantly shortened relative to those of the hydrogen-bridged B6−B7, B8−B9 and B9−B10 borons. The B5−B10 distance in **5Cl**$^-$ (1.844(3) Å) is also considerably shortened relative to its corresponding B7−B8 distance (2.208(3) Å). The B5−Cl distance in **5Cl**$^-$ (1.844(2) Å) is significantly longer than the B6−Cl distance in **6Cl**$^-$ (1.811(2) Å) with both of the distances being longer than the B6−Cl distance of **6Cl** (1.764(2) Å)[3]

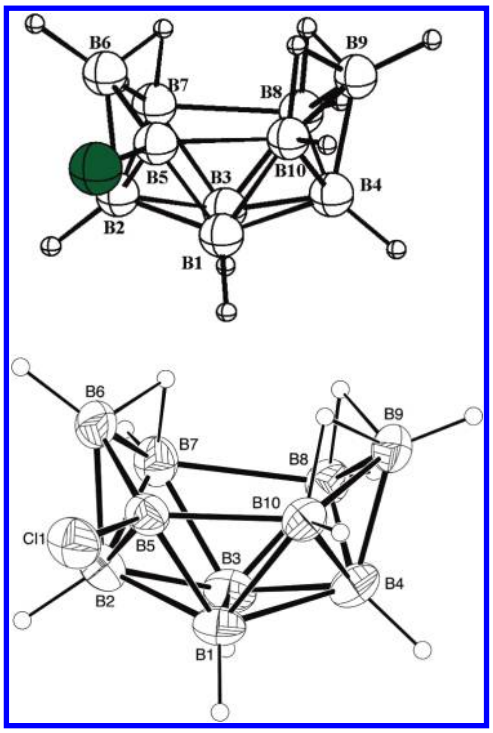

Figure 5. (top) DFT (B3LYP/6-311G(d)) optimized geometry and (bottom) crystallographically determined structure of **5Cl**$^-$. Selected bond lengths (Å) and bond angles (deg): (**top**) B5−Cl, 1.867; B5−B6, 1.652; B6−B7, 1.787; B7−B8, 2.052; B8−B9, 1.786; B9−B10, 1.797; B10−B5, 1.860; B6−B2, 1.767; B9−B4, 1.710; B2−B5, 1.805; B2−B7, 1.768; B1−B5, 1.739; B1−B10, 1.797; B1−B4, 1.807; B3−B7, 1.775; B3−B8, 1.739; B1−B3, 1.801; Cl−B5−B2, 124.08; B7−B6−B5, 107.12; B8−B9−B10, 103.94; Cl−B5−B1, 118.00; Cl−B5−B6, 121.26; B6−B5−B10, 113.78; B6−B7−B8, 115.44; B7−B8−B9, 112.52; B5−B10−B9, 122.77. (**bottom**) B5−Cl, 1.844(2); B5−B6, 1.644(3); B6−B7, 1.775(3); B7−B8, 2.028(3); B8−B9, 1.773(3); B9−B10, 1.791(3); B10−B5, 1.844(3): B6−B2, 1.754(3); B9−B4, 1.702(3); B2−B5, 1.790(3); B2−B7, 1.764(3); B1−B5, 1.737(3); B1−B10, 1.796(3); B1−B4, 1.804(3); B3−B7, 1.770(3); B3−B8, 1.737(3); B1−B3, 1.787(3); Cl−B5−B2, 124.80(13); B7−B6−B5, 106.75(16); B8−B9−B10, 103.96(15); Cl−B5−B1, 117.67(13); Cl−B5−B6, 121.75(14); B6−B5−B10, 113.82(15); B6−B7−B8, 116.19(15); B7−B8−B9, 112.06(14); B5−B10−B9, 122.59(15).

(21) Fujii, T.; Nishida, H.; Abiru, Y.; Yamamato, M.; Kise, M. *Chem. Pharm. Bull.* **1995**, *43*, 1872–1877.
(22) Bos, M.; Dahmen, E. A. M. F. *Anal. Chim. Acta* **1973**, *63*, 185–196.
(23) Alder, R. W.; Bowman, P. S.; Steele, W. R. S.; Winterman, D. R. *Chem. Commun.* **1968**, 723–724.
(24) Sneddon, L. G.; Huffman, J. C.; Schaeffer, R. O.; Streib, W. E. *Chem. Commun.* **1972**, 474–475.
(25) Wynd, A. J.; Welch, A. J. *Acta Crystallogr.* **1989**, *C45*, 615–617.

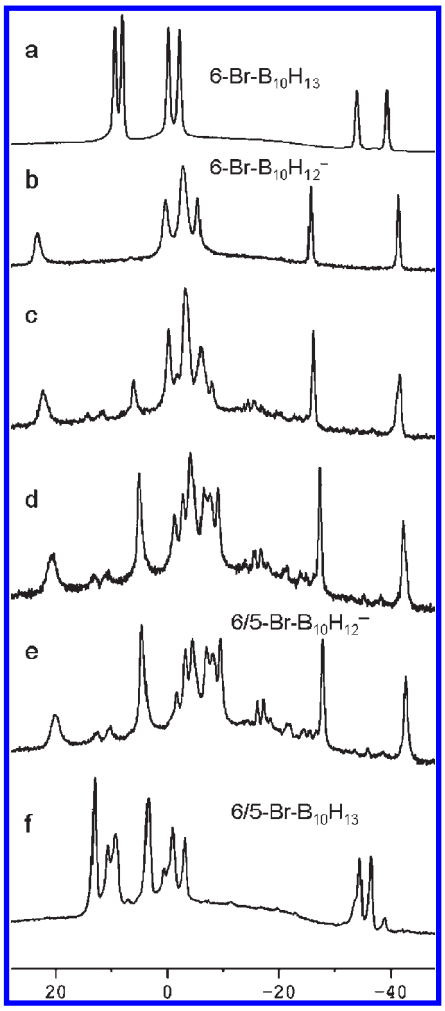

Figure 6. Deprotonation of **6Br** and isomerization of resultant **6Br**$^-$ at 60 °C in dichlorobenzene monitored by $^{11}B\{^1H\}$ NMR. (**a**) **6Br**, (**b**) **6Br**$^-$, 0 min; (**c**) 60 min; (**d**) 90 min; (**e**) 130 min; (**f**) acidified mixture after 130 min.

suggesting reduced Cl to B π back-donation in the more electron-rich anions.

Figure 6a shows the ^{11}B NMR spectrum of **6Br**, while Figure 6b is that of **6Br**$^-$ resulting from its reaction with 1 equiv of PS. The **6Br**$^-$ solution was held at 60 °C in dichlorobenzene, and its isomerization to **5Br**$^-$ monitored over time. Since the 6B resonance in **6Br**$^-$ and the 5B resonance in **5Br**$^-$ are coincident (~25 ppm), the progress of the isomerization can be most easily followed through the appearance of the 4.5 ppm resonance of **5Br**$^-$ along with the corresponding disappearance of the −2.0 ppm resonance of **6Br**$^-$. After 90 min at 60 °C, equal amounts of the two anions were present (Figure 6d), and after 130 min, no further change in their relative amounts was observed (Figure 6e). Acidification at this point yielded same ~82:18 **5Br**/**6Br** ratio mixture that was found for the **6Br** isomerizations catalyzed with TEA (Figure 6f).

The DFT calculated free energies for 6-X-$B_{10}H_{12}^-$ isomerization to 5-X-$B_{10}H_{12}^-$ at 60 °C (Figure 7) range from a positive value for **6F**$^-$, to progressively more negative values as the halogen is changed from Cl to Br to I. This trend is consistent with the experimental results, in that the TEA-catalyzed reaction of **6F** gave only trace

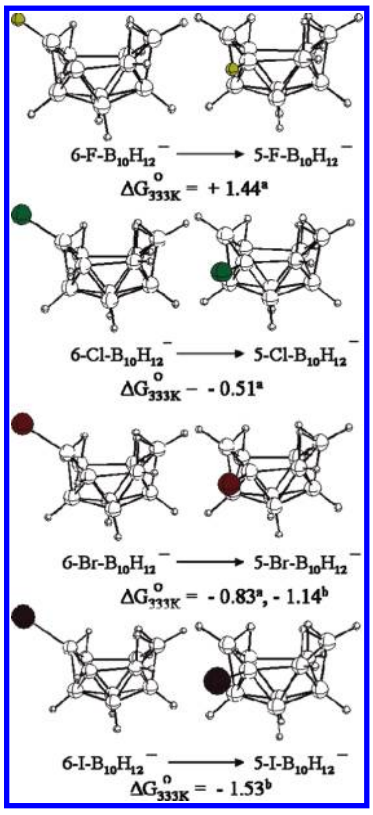

Figure 7. DFT optimized geometries of 6-X- and 5-X-$B_{10}H_{12}^-$ and calculated free energy changes in their isomerizations at 60 °C. [a]Optimization and free energy calculation at B3LYP/6-311G(d). [b]Optimization and free energy calculation used B3LYP/6-311G(d) for all H and B atoms, and the SDD pseudopotential for Br and I.

Table 2. Calculated and Observed Equilibrium Constants for the Isomerization of 6-X-$B_{10}H_{12}^-$ to 5-X-$B_{10}H_{12}^-$ at 60 °C[a]

X-$B_{10}H_{13}$	K_{calc} [5X$^-$]/[6X$^-$]	K_{obs} [5X]/[6X]
F	0.1[b]	< 0.05
Cl	2.2[b]	3.5
Br	3.4[b]	4.9
	5.6[c]	
I	10.1[c]	6.1
6-R-X-$B_{10}H_{12}$[d]		
Cl	2.2[b]	2.9
I	23.2[c]	6.9
6-R-$B_{10}H_{13}$[d]	3.9×10^{-2}[b]	0
6,9-R_2-$B_{10}H_{12}$[d]	0.1[b]	0

[a] Calculated K values are derived from the DFT calculated ΔG^o of reaction at 60 °C. [b] B3LYP/6-311G(d) level for all atoms. [c] B3LYP/6-311G(d) level for H, C, and B atoms and the SDD pseudopotential for I. [d] R = C_2H_5 in calculated values, R = C_6H_{13} in observed values.

isomerization, while the reactions of **6Cl**, **6Br**, and **6I** gave progressively higher equilibrium **5X**/**6X** ratios. In fact, as indicated in Table 2, the equilibrium constant values obtained from the calculated free energies of isomerization of these anions agree quite well with the experimentally observed values both in scale and trend ($K_I > K_{Br} > K_{Cl} > K_F$). Thus, both these calculations and the NMR study in Figure 6 strongly support a mechanistic pathway (Figure 8) for the base-catalyzed **6X** to **5X** conversions involving formation and subsequent isomerization of the **6X**$^-$ anions with the final **5X**/**6X** equilibrium ratios determined by the energetic differences of their corresponding 6-X-$B_{10}H_{12}^-$ and 5-X-$B_{10}H_{12}^-$ anions.

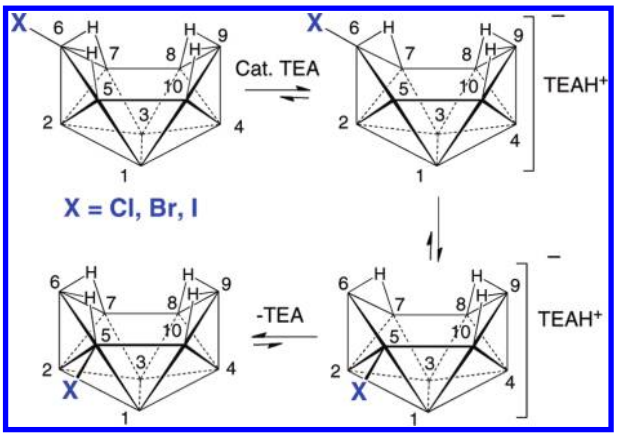

Figure 8. Proposed pathway for the base-catalyzed isomerization of **6X** compounds.

Isomerization of 6-X-9-R-$B_{10}H_{12}$. In agreement with the DFT calculations of the relative energies of 6 and 5-substituted alkyl-isomers (Table 2), neither 6-(C_6H_{13})-$B_{10}H_{13}$ nor 6,9-(C_6H_{13})$_2$-$B_{10}H_{12}$ isomerized when reacted with 5% TEA at 60 °C (eq 4). However, when either 6-Cl-9-(C_6H_{13})-$B_{10}H_{12}$ or 6-I-9-(C_6H_{13})-$B_{10}H_{12}$ were treated with 5% TEA in toluene at 60 °C (eq 5), their ^{11}B NMR (Figure 9) spectra showed the emergence of new C_1-symmetric species.

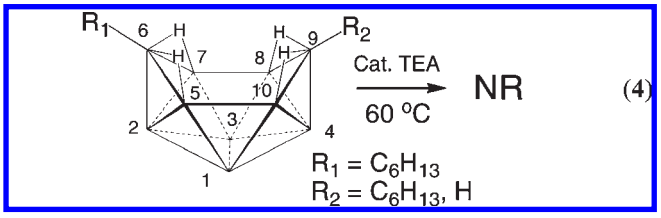

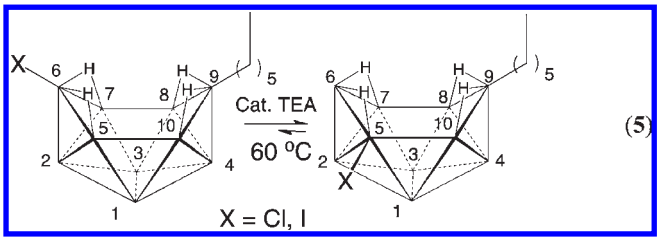

In principle, several different isomers resulting from either halo or alkyl migration could have formed, but DFT optimizations of the possible isomers showed that 5-X-9-R-$B_{10}H_{12}$ products (**5X-9R**) were energetically favored with the DFT/GIAO calculated chemical shifts for the model compound 5-Cl-9-(C_2H_5)-$B_{10}H_{12}$ being in excellent agreement with the experimentally observed shifts for 5-Cl-9-(C_6H_{13})-$B_{10}H_{12}$. In both reactions, equilibrium mixtures of the **5X-9R** and **6X-9R** isomers were formed with the experimentally observed ~3:1 (X = Cl) and ~7:1 (X = I) **5X-9R**/**6X-9R** equilibrium ratios again consistent with the DFT calculated differences in the free energies of the **5X-9Et**$^-$ and **6X-9Et**$^-$ model compounds (Figure 10).

Our computational investigations of their rearrangement mechanisms have not yet yielded isomerization pathways from **6X**$^-$ to **5X**$^-$ or from **6X-9R**$^-$ to **5X-9R**$^-$ that would be energetically feasible at 60 °C. The usual

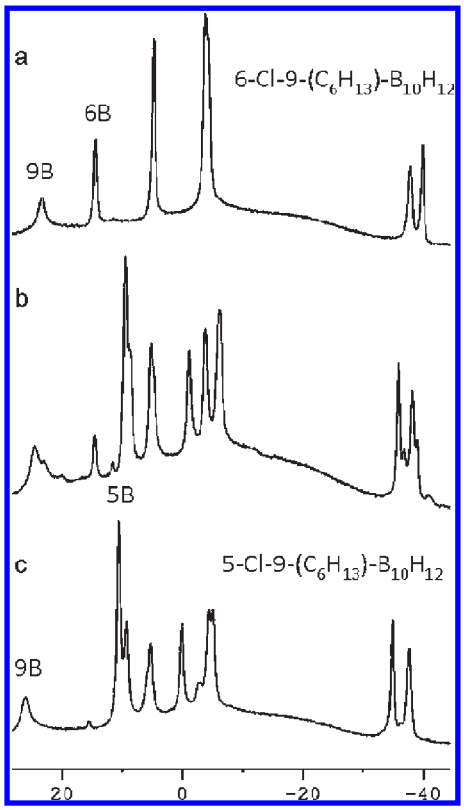

Figure 9. Isomerization of 6-Cl-9-(C_6H_{13})-$B_{10}H_{12}$ in toluene monitored by $^{11}B\{^1H\}$ NMR. (**a**) 6-Cl-(C_6H_{13})-$B_{10}H_{12}$ before base addition. (**b**) reaction mixture of 6-Cl-9-(C_6H_{13})-$B_{10}H_{12}$ and 5-Cl-9-(C_6H_{13})-$B_{10}H_{12}$ produced after 4 h at 60 °C. (**c**) 5-Cl-9-(C_6H_{13})-$B_{10}H_{12}$ isomer after column purification (spectrum taken in $CDCl_3$). Substituted boron peaks are labeled (singlet at 11.4 ppm is coincident with another resonance in (c)). DFT/GIAO calculated ^{11}B NMR shifts for the 5-Cl-9-(C_2H_5)-$B_{10}H_{12}$ model compound: 25.0 (B9), 14.5 (B5), 13.0 (B3), 11.0 (B1), 3.0 (B6), 1.9 (B10), −4.0 (B8), −4.5 (B7), −37.8 (B4), −39.5 (B2).

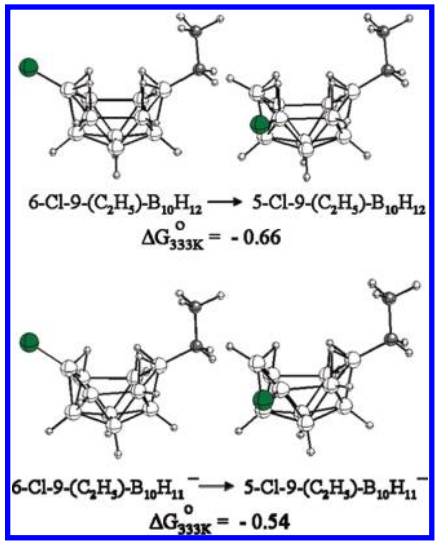

Figure 10. DFT optimized geometries and calculated free energy changes at B3LYP/6-311G(d) for the isomerizations at 60 °C of (top) 6-Cl-9-(C_2H_5)-$B_{10}H_{12}$ and 5-Cl-9-(C_2H_5)-$B_{10}H_{12}$ and (bottom) 6-Cl-9-(C_2H_5)-$B_{10}H_{11}^-$ and 5-Cl-9-(C_2H_5)-$B_{10}H_{11}^-$.

mechanisms postulated to account for halo- or alkyl-isomerizations in polyhedral boranes and carboranes have involved skeletal rearrangements where the halo- or alkyl-substituent remains attached to its skeletal-boron during

the isomerization. However, our computational investigations of the standard[26] skeletal-based rearrangement mechanisms, including trigonal face rotation (TFR), pentagonal face rotation (PFR), and diamond-square-diamond (DSD) transformations, have not been successful in identifying viable pathways for skeletal-rearrangement. Furthermore, energy calculations predict that a distribution of isomers, where the alkyl or halogen had migrated to other cage positions, would be produced by these skeletal-rearrangements, but these isomers were not observed experimentally. The fact that no I to Cl exchange was observed when the isomerization of **6I** to **5I** was carried out in the presence of $Bu_4N^+Cl^-$ would also seem to exclude any halo-dissociative mechanism. At this point, the combined computational and experimental results suggest a mechanism for the **6X**$^-$ to **5X**$^-$ and **6X-9R**$^-$ to **5X-9R**$^-$ isomerizations with direct transfer of the halogen from B6 to B5, perhaps involving a halogen bridging the deprotonated B5−B6 edge, may be possible. We are continuing to computationally explore these and other possibilities.

Fluxional Properties of the 6-X-$B_{10}H_{12}^-$ Anions. The DFT/GIAO calculated ^{11}B NMR chemical shifts for the **5Cl**$^-$ structure in Figure 5a match well the experimental chemical shifts observed over the −53 to 102 °C range (obs/cal): B6 (19.0/18.6), B5 (10.5/14.8), B1 (4.0/5.5), B3 (−3.8/−5.4), B8 (−4.8/−5.6), B10 (−7.1/−7.4), B7 (−7.9/−12.4), B9 (−10.1/−14.3), B2 (−27.6/−28.7) and B4 (−42.9/−47.5). At lower temperatures, the spectra observed for **6Cl**$^-$ (12 °C) and **6F**$^-$ (27 °C) likewise match the GIAO calculated chemical shifts (Tables 3 and 4) for their DFT-optimized C_1-symmetric structures given in Figures 4a and 7. However, the ^{11}B NMR spectra of **6Cl**$^-$ and **6F**$^-$ changed as the temperature was increased, with the spectra observed at higher temperatures consistent with C_s-symmetric structures. Thus, the spectrum of **6Cl**$^-$ at 32 °C (Figure 11) showed only the four sharp intensity-one resonances arising from the B2, B4, B6, and B9 borons, along with a single broad resonance of intensity 6 centered near −1 ppm. Upon raising the temperature to 67 °C, the broad resonance narrowed and resolved into three new intensity-two sharp peaks. A similar dynamic behavior was observed in the ^{11}B NMR spectra of **6F**$^-$ (Figure 12) where at 67 °C the spectrum began to broaden and then at 97 °C, 6 of the original 10 sharp peaks were replaced by 2 new broad peaks centered at −6.1 ppm (intensity 4) and −15.0 ppm (intensity 2).

The temperature dependent spectra observed for **6Cl**$^-$ and **6F**$^-$ suggest fluxional behavior, such as has been observed in the parent $B_{10}H_{13}^-$, involving hydrogen migration around the open face that then leads to the averaging of some boron resonances at higher temperatures. While a solid-state C_1 symmetric structure was also established for $B_{10}H_{13}^-$, its solution ^{11}B NMR spectrum was reported to show only four resonances in 2:1:5:2 ratios suggesting C_s-symmetry on the NMR time scale.[27] This apparent conflict was resolved by Hofmann and

Table 3. Comparisons of the DFT/GIAO (B3LYP/6-311G(d)) Calculated and Experimentally Observed Chemical Shifts in the ^{11}B NMR Spectra of **6Cl**$^-$ [a]

Observed 12 °C	Calculated C_1-Structure	Observed 67 °C	C_1-Averaged C_s-Pattern
27.6	30.1 (B6)	27.9	30.1 (B6)
0.6	1.9 (B1)	-2.4(2)	-2.1 (B1,3)
-1.7	-3.4 (B5)		
-4.0	-3.5 (B8)	-4.6(2)	-7.4 (B5,7)
-5.6	-6.1 (B3)		
-8.1(2)	-8.4 (B10)	-6.3(2)	-6.0 (B8,10)
	-11.4 (B7)		
-9.9	-14.0 (B9)	-8.1	-14.0 (B9)
-26.6	-27.5 (B2)	-26.3	-27.5 (B2)
-43.6	-46.4 (B4)	-43.5	-46.4 (B4)

[a] Colors indicate which boron resonances are averaged.

Table 4. Comparisons of the DFT/GIAO (B3LYP/6-311G(d)) Calculated and Experimentally Observed Chemical Shifts in the ^{11}B NMR Spectra of **6F**$^-$ [a]

Observed 27 °C	Calculated C_1-Structure	Observed 97 °C	C_1-Averaged C_s-Pattern
34.9	34.5 (B6)	34.9	34.5 (B6)
-1.2	-3.2 (B8)		
-4.4	-3.5 (B1)	-5.9(4)	-5.0 (B8,10)
-6.9	-6.8 (B10)		-5.7 (B1,3)
-7.9	-7.9 (B3)		
-11.8	-13.8 (B5)	-11.8	-18.1 (B9)
-12.6	-18.1 (B9)	-15.0(2)	-17.0 (B5,7)
-17.4	-20.2 (B7)		
-25.6	-26.3 (B2)	-25.4	-26.3 (B2)
-46.6	-49.3 (B4)	-46.5	-49.3 (B4)

[a] Colors indicate which boron resonances are averaged (bold face entries).

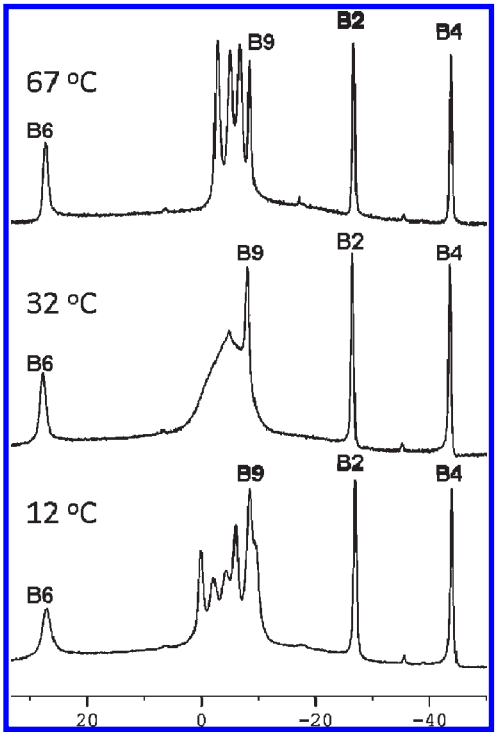

Figure 11. Variable temperature ^{11}B{^{1}H} NMR spectra of **6Cl**$^-$.

(26) (a) Lipscomb, W. N. *Science* **1966**, *153*, 373–378. (b) Wu, S-h.; Jones, M., Jr. *J. Am. Chem. Soc.* **1989**, *111*, 5373–5384. (c) Gimarc, B. M.; Ott, J. J. *J. Am. Chem. Soc.* **1987**, *109*, 1388–1392. (d) Gimarc, B. M.; Warren, D. S.; Ott, J. J.; Brown, C. *Inorg. Chem.* **1991**, *30*, 1598–1605. (e) Wales, D. J. *J. Am. Chem. Soc.* **1993**, *115*, 1557–1567. (f) Hart, H. V.; Lipscomb, W. N. *J. Am. Chem. Soc.* **1969**, *91*, 771–772. (g) Kaesz, H. D.; Bau, R.; Beall, H. A.; Lipscomb, W. N. *J. Am. Chem. Soc.* **1967**, *89*, 4218–4220. (h) Edvenson, G. M.; Gaines, D. F. *Inorg. Chem.* **1990**, *29*, 1210−1216 and references therein.

(27) Siedle, A. R.; Bodner, G. M.; Todd, L. J. *J. Inorg. Nucl. Chem.* **1971**, *33*, 3671–3676.

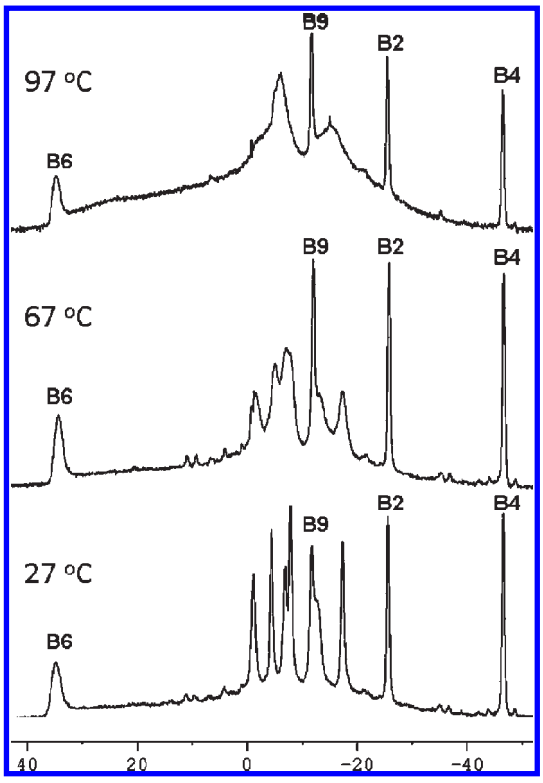

Figure 12. Variable temperature $^{11}B\{^{1}H\}$ NMR spectra of $\mathbf{6F}^-$.

Schleyer's computational studies (MP2/6-31G(d) level),[28] which showed that while the C_1 structure is 4.5 kcal/mol lower in energy than the C_s structure, the C_s symmetric pattern observed in the NMR could be explained by a fluxional hydrogen rearrangement which interconverts the two enantiomeric forms of the C_1 structure. Averaging the chemical shifts for the boron atoms in the C_1 structure that become equivalent in the fluxional structure then gave good agreement with the experimental spectrum.

DFT calculations identified the two pathways shown in Figure 13 for hydrogen-migration in $\mathbf{6Cl}^-$ and $\mathbf{6F}^-$. The top pathway is similar to that proposed by Schleyer for $B_{10}H_{13}^-$, involving hydrogen-migration along only one side of the cage by a process in which a single bridge-hydrogen migrates across the B6−B5, B5−B10, and B10−B9 edges via the *endo*-B5-H (TS1) and *endo*-B10-H (TS2) transition states and the B5−H−B10 intermediate (Int1). The low barrier for this process supports its occurrence in $\mathbf{6Cl}^-$ (7.9 kcal/mol) and $\mathbf{6F}^-$ (6.9 kcal/mol); however, owing to the lower symmetry of the 6-X-$B_{10}H_{12}^-$ anions, such a process, unlike in the parent $B_{10}H_{13}^-$, will not average to give a C_s-symmetric ^{11}B NMR spectrum

A second pathway for hydrogen migration, involving the movement of one bridging-hydrogen from the B6−B7 edge to its enantiomeric position on the B5−B6 edge is shown at the bottom of Figure 13. While the barrier going through the TS3 transition state structure, which has an *endo*-hydrogen at B6, is higher in $\mathbf{6Cl}^-$ (12.5 kcal) and $\mathbf{6F}^-$ (16.7 kcal) than that of the first process, this barrier should still be accessible at the experimentally observed

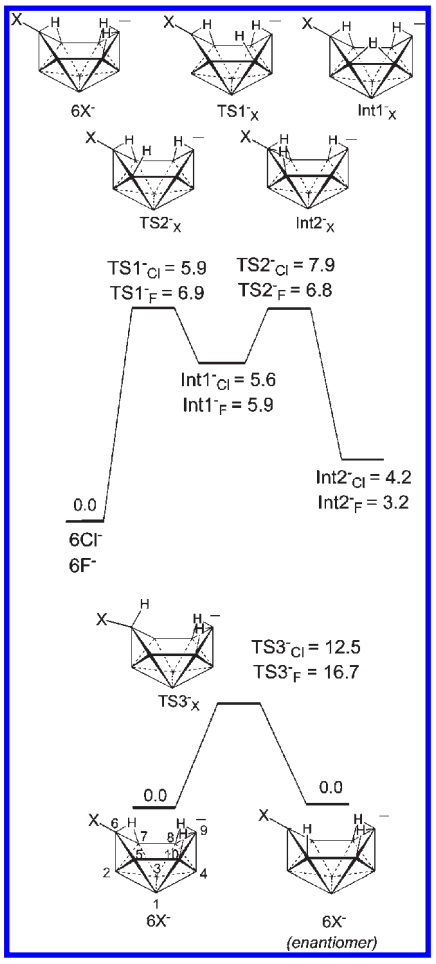

Figure 13. Calculated relative electronic energies (B3LYP/6-311G(d)) at 293.15 K for two hydrogen migration pathways in $\mathbf{6X}^-$ (X = Cl, F).

temperatures of fluxionality and, in the fast exchange limit, this process would produce a C_s-symmetric ^{11}B NMR spectrum. As shown in Tables 3 and 4, averaging the calculated shifts of the B5−B7, B10−B8 and B1−B3 pairs of boron atoms that would become equivalent in this process does indeed give excellent agreement with the values observed in the higher temperature spectra of $\mathbf{6Cl}^-$ and $\mathbf{6F}^-$. The relative barriers calculated for this process for $\mathbf{6Cl}^-$ and $\mathbf{6F}^-$ are likewise in agreement with the lower temperature required for $\mathbf{6Cl}^-$ to reach the fast exchange limit.

In conclusion, the new methods reported herein for the syntheses of the 5-X-$B_{10}H_{13}$ halodecaboranes from their 6-X-$B_{10}H_{13}$ isomers, coupled with our previous development of high yield routes to the 6-X-$B_{10}H_{13}$ compounds from the cage-opening reactions of *closo*-$B_{10}H_{10}^{2-}$ salts, now provide the first efficient routes to these synthetically useful decaborane derivatives. These syntheses are now enabling the first systematic investigations of halodecaborane reactivities, and our initial studies[29] have demonstrated that halodecaboranes readily undergo high yield transformations to a wide variety of functional decaborane derivatives of potential interest for either biomedical or materials applications. These studies, as well as further computational and experimental investigations of the unique mechanism(s) by which the halo rearrangement

(28) Hofmann, M.; Schleyer, P. v. R. *Inorg. Chem.* **1998**, *37*, 5557–5565.

(29) Ewing, W. C.; Carroll, P. J.; Sneddon, L. G. work in progress.

occurs in the 6-X-$B_{10}H_{13}$ to 5-X-$B_{10}H_{13}$ isomerizations, will be reported in future publications.

Acknowledgment. We thank the National Science Foundation and the U.S. Department of Energy for support.

Supporting Information Available: Tables listing Cartesian coordinates and calculated energies for DFT-optimized geometries; tables of IR data; and CIF files for **5I**, **5Br**, **6Cl**$^-$, and **5Cl**$^-$. This material is available free of charge via the Internet at http://pubs.acs.org.